Effect of Addition of Oligobetapinene on Morphology, Thermal and Gas Permeation Properties in Blends with HDPE

Luis C. Mendes,[1] Lívia F. C. Jatobá,[1] Anderson F. Ferreira,[1] Maria E. F. Garcia[2]

[1]*Instituto de Macromoléculas Professora Eloisa Mano (IMA), Universidade Federal do Rio de Janeiro (UFRJ), Centro de Tecnologia, Bloco J, P.O. Box 68525, 21945-970, Rio de Janeiro, RJ, Brazil*
[2]*Coordenação dos Programas de Pos-Graduação em Engenharia, COPPE/UFRJ, Programa de Engenharia Química (PEQ)*

Received 25 January 2003; revised 15 March 2003; accepted 25 May 2003

ABSTRACT: Binary blends of high density polyethylene (HDPE) and oligobetapinene (OBP) were prepared by melt mixing. The morphology, thermal and permeability properties of compression molded and slow cooled films are reported. Applying the first-derivative procedure on differential scanning calorimetry (DSC) traces, we have detected the temperature of glass transition (T_g) of HDPE as a large peak centered from −125 to −100°C. In the blends, we observed that the OBP molecules were able to resolve the transition into two components. The lower one was ascribed to the γ-transition of HDPE, and the upper one was attributed to its T_g. The OBP molecules also formed another transition at a higher temperature. The blends were composed at least of three distinct phases, likely composed of amorphous HDPE with some amount of OBP molecules, amorphous OBP with some polyolefin and crystalline HDPE. The scanning electron microscopy (SEM) investigations revealed segregation of the components. The permeation to CO_2 of plain HDPE and 90/10 blends was similar, but at higher concentrations of oligomer, the value was slightly higher than that of neat HDPE. The decrease of overall crystallinity was counterbalanced by the presence of an OBP rich phase in the blend and could explain the slight increase in permeability of the film blends. J Appl Polym Sci 91: 315–320, 2004

Key words: polyethylene; thermal properties; blends

INTRODUCTION

Among the polyolefins, high density polyethylene (HDPE) is a thermoplastic with various applications. It represents the fourth thermoplastic most commonly sold around the world due to properties such as processability, impact and chemical resistance. With respect to processing, it can be conformed by injection, extrusion and blow molding processes, producing bottles, films, sheets, pipes, cables, etc. Its large applicability in the package industry makes it the second most recycled resin in the world. Its properties can be modified by blending with other polymers or by the addition of a second component of low molecular weight. Commonly added mineral resins include cumarone-indene, aliphatic and aromatic hydrocarbons and natural resins such as rosin, modified rosin and terpenes, which can generate interesting changes in blend properties when blended with polymers.[1–4] Their applications include use as a tackifier agent in adhesive compositions. Kajiyama[5] and coworkers have studied the effect on shear, tensile, peel and creep strength of a type of terpene phenol oligomer used as a tackifier agent for a hot-melt adhesive based on a copolymer of ethylene and vinyl acetate (EVA). The adhesive, phase behavior, miscibility and viscoelastic properties of blends of elastomers with a type of hydrogenated (vinyl toluene)/indene oligomer resin for adhesive applications were studied by Kim and coworkers.[6-7] Akiyama[8] has investigated the phase behavior of a mixture of poly(styrene-*b*-isoprene-*b*-styrene)(SIS)/hydrogenated terpene resin using thermal analysis, morphological observation and cloud point.

The mixture of polyolefins and oligoresins is the subject of our and other research groups aiming to correlate changes in phase structure, morphology, thermal behavior, rheology, crystallization, mechanical and permeation properties with the addition of such low molecular mass resins. Binary and ternary systems of HDPE, polypropylene (PP) and hydrogenated oligo(cyclopentadiene) (HOCP) were prepared in the molten state, and their phase structure, thermal behavior, morphology, mechanical properties and crystallization are reported.[9–12] The influence of the addition of a glycerol ester of hydrogenated rosin (ester gum) on the morphology, mechanical and rheological properties and the thermal and viscoelastic

Correspondence to: L. C. Mendes (lcmendes@ima.ufrj.br).

Journal of Applied Polymer Science, Vol. 91, 315–320 (2004)

behavior of HDPE was studied.[13-14] The authors have concluded that all blends formed phase segregated systems. Melt blends of PP and ester gum under select conditions were prepared.[15–17] The crystallization results indicate changes in the radial growth rate and size of PP spherulites, and the mechanical properties varied with the amount of ester gum added. The solid state ^{13}C-NMR study of proton spin lattice relaxation time in the rotating frame ($T_1{}^H\rho$) of this system has revealed the enhancement of mobility of PP and suggests sample homogeneity. Poly(α-pinene) and poly(*d*-limonene), two natural oligoresins, were blended with PP, and the effects on crystallization growth rates, phase structure, thermal and viscoelastic properties are discussed.[18-19] Thermal properties and phase structure of compression molded plaques of PP and oligobetapinene blends were studied using differential scanning calorimetry (DSC), scanning electron microscopy (SEM) and optical microscopy techniques.[20] The results indicate that the system is an immiscible blend that forms at least two amorphous phases and one crystalline phase. Another article on PP/oligobetapinene (OBP) systems reports the increase of hardness, density and elastic modulus and the decrease of torque with OBP concentration.[21] Recently, an article reporting the mechanical, thermal and gas permeation properties of PP/OBP systems was accepted for publication.[22]

We are attempting to modify the mechanical, adhesive, permeability and sealing properties of polyolefins by blending them with low molar mass resins. In this study, our interest was mainly the preparation of thin films of HDPE and OBP blends under different conditions and the evaluation of variations in permeability, viewing its use as packing material. In addition, we also evaluated the morphology and thermal properties of the films.

EXPERIMENTAL

Materials

HDPE, grade BT 003, was kindly supplied by Polialden, Brazil. The density was 967 kg/m^3,[23] according to ASTM D 792; the degree of crystallinity and melt flow index were 63% and 0.3 g/10 min, respectively.

OBP was manufactured by Cloral S/A, Brazil. This resin is obtained through the polymerization reaction of β-pinene, a natural cyclic monomer, using a cationic process. The resulting resin is a low molecular weight product whose repeating unit can be viewed as an alternating copolymer of isobutylene and cyclohexene.[4] The resin has a yellowish, amorphous aspect, with average weights of M_n = 570 and M_w = 920, calculated by GPC, and a density[23] of 988 kg/m^3.

Blend preparation

Mixtures of HDPE and OBP were prepared in a Haake Rheocord 9000 equipped with an internal mixer, in molten state at 200°C, 30 rpm for 5 min. The blend nominal ratios were 100/0, 90/10, 80/20, 70/30, 60/40 and 50/50.

Film preparation

Films were produced in a Carver press at 200°C, where the mixtures were left for 1 min for softening; then 50 a kN load was applied during 4 min to conform the films. From the molten state, the films were cooled at an average cooling rate of 15°C/min until they reached room temperature. The average thickness of the films was 0.01 cm.

Permeation test

CO_2 permeation through the polymeric films was measured using a traditional gas permeability analyzer.[24] The permeation cell consists of two stainless steel compartments separated by the membrane under study. The gas was fed at a constant pressure (10^5 N/m^2) into the bottom cell, and the amount of gas passing through the membrane was measured by the pressure increase on the downstream side with a pressure transducer. At a steady gas flow, the permeability (P/l) was determined from the slope (dp/dt) of the pressure versus time plot using the following equation:[25]

$$\frac{P}{l} = \frac{dp}{dt}\left(\frac{V_{\text{system}}}{A\Delta p}\right)\left(\frac{T_{\text{STP}}}{T_{\text{ambiens}}P_{\text{STP}}}\right)$$

where P is the permeability coefficient, l is the film thickness, dp/dt is the slope of the pressure versus time plot, V_{system} is the volume of the system, A is the film area, Δp is the pressure difference between the two sides of the film, T_{STP} is the absolute temperature of 273 K, T_{ambient} is the temperature of the test (296 K), and P_{STP} is the absolute pressure of 76 cm Hg.

DSC analysis

The thermal analysis of the films was carried out in a Perkin–Elmer DSC 7 calorimeter equipped with a data acquisition system and a computer program for calculation. About 10 mg of each sample were placed in an aluminum pan and tested from −150 to 0°C and 0 to 170°C at 10°C/min. The glass transition and melting temperatures (T_g and T_m) were taken from the DSC curves. The crystallinity degree (X_c) was evaluated considering the melting enthalpy for each mixture and the melting enthalpy of 100% crystalline HDPE[26] to be ΔH^0 = 290 J/g. The crystallinity data

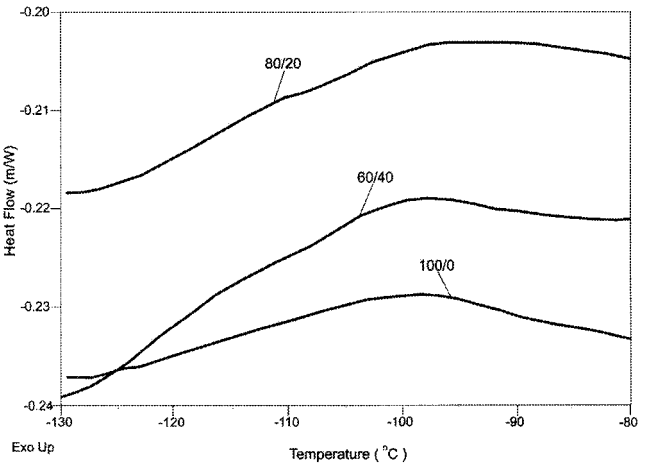

Figure 1 DSC traces of HDPE/OBP films from −130 to −80°C.

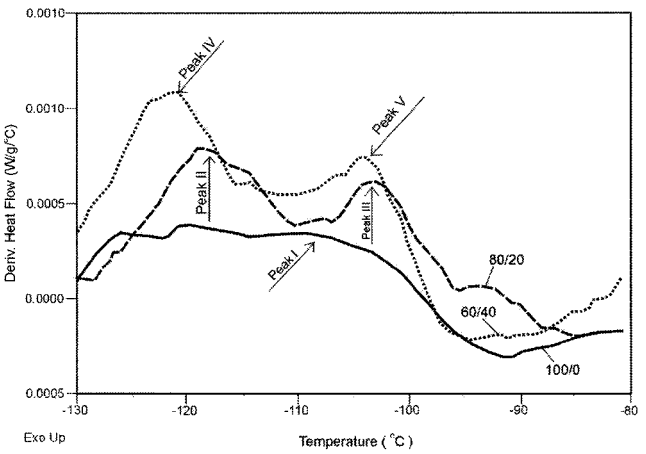

Figure 2 Derived function of DSC traces of HDPE/OBP films from −130 to −80°C.

were normalized with respect to the HDPE content for each blend.

Morphological analysis

Morphology evaluation was carried out using a scanning electron microscope JEOL JMS 5610 LV. A small specimen was cut from the molded film and fractured after freezing (for 30 min) in liquid nitrogen. The fractured piece was sputtered with a thin layer of gold/palladium alloy before SEM observation.

RESULTS AND DISCUSSION

The DSC curves were evaluated considering the temperature intervals of the glass transition of HDPE (−150 to 0°C), the glass transition of OBP and the melting peak of HDPE (0 to 170°C).

Thermograms of neat HDPE, 80/20 and 60/40 HDPE/OBP films from −130 to −80°C are presented in Figure 1. The DSC curves show some similarity. The trace of neat HDPE seems to show a unique transition, while the 60/40 HDPE/OBP trace is divided into two distinct components. The derived function was applied to the DSC traces, and the results reported in Figure 2. The DSC first-derivative curve of plain HDPE shows a broad peak located between −125 and −100°C (Peak I), considered here to be the T_g of HDPE. For the blends, the first-derivative curves clearly show two peaks. For the 80/20 HDPE/OBP blend, there is one peak centered at about −125 to −110°C (Peak II), with a maximum at −118°C and another peak at a higher temperature of about −108 to −100°C (Peak III), with a maximum at −103°C. For the 60/40 HDPE/OBP blend, there are also two peaks. The lower one appears between −128 and −115°C (Peak IV), with a maximum at −122°C, while the upper one is located between −108 and −100°C (Peak V), with a maximum located at −105°C. Although the transitions of HDPE have been studied extensively using several experimental methods, there is still controversy regarding its assignment and molecular origin. This is particularly true for its main T_g, which is normally assigned a large temperature interval (−130 to −20°C).[27] The presence of OBP molecules provokes some disturbance in the amorphous phase of HDPE, evidenced by the deconvoluting of the first-derivative curve in the region of its T_g. For both blends, based on the results, we could consider that the peak at the lowest temperature corresponds to the γ-transition of HDPE and the one at the highest temperature corresponds to its T_g. Our results are somewhat similar to those previously published by Lee & Simha[28] and Stehling & Mandelkern,[29] in that the T_g of HDPE is composed of two components and is localized in the γ-transition region.

Figure 3 shows the calorimetric curves of neat HDPE and OBP, and of 90/10, 80/20 and 60/40 HDPE/OBP films from 0 to 170°C. The melting peak of HDPE was observed, indicating that crystallization

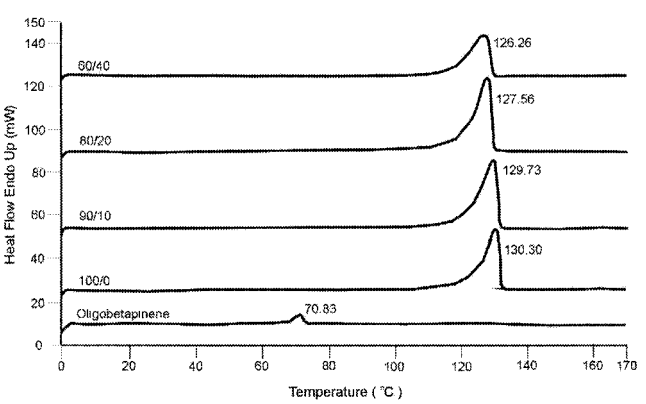

Figure 3 DSC traces of HDPE/OBP films from 0 to 170°C.

TABLE I
Calorimetric Parameters for HDPE/OBP Films from 0 to 170°C

HDPE/OBP	T_m (°C)	χ_b (%)	χ_c (%)
100/0	130	64	64
90/10	130	55	61
80/20	128	51	64
60/40	126	40	67

T_m = melting temperature; χ_b = blend crystallinity; χ_c = HDPE normalized crystallinity.

occurs in all blend compositions. Table I summarizes the melting points and crystallinity indices of these blends. The slight decrease in melting temperature could be explained by the formation of more defective HDPE crystals in the presence of oligomer molecules. The crystallinity indices of the blends decreased with the amount of OBP, but when it was normalized with respect to HDPE the values found were similar, except for the 60/40 blend, which was slightly higher. The neat OBP curve showed a peak at about 71°C. This peak disappeared when the sample was reheated, showing a baseline variation similar to the glass transition of polymers. This transition was attributed to the T_g of OBP, in agreement with the value found in the literature.[5,8,18–22]

The DSC traces of neat HDPE, 90/10, 80/20 and 60/40 blends in the region of the T_g of OBP (0 to 100°C) are shown in Figure 4. At 30 to 40°C, there is a slight inflection of the HDPE curve that could be assigned to its α-relaxation concerning the mobility of chain segments in the crystal region.[30] In the case of the blends, the thermal curves show baseline variation at 40 to 50°C. We have ascribed this to the T_g of the amorphous OBP rich phase. The T_g calculations were completed using a computer program for DSC equipment, and the values appear in Table II. The values are practically equal and independent of OBP content.

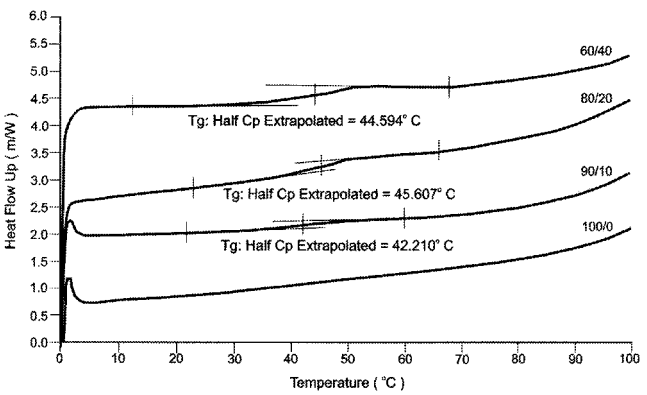

Figure 4 DSC traces of HDPE/OBP films from 0 to 100°C.

TABLE II
T_g of Oligobetapinene Rich Phase of HDPE/OBP Films from 0 to 100°C

HDPE/OBP	T_g (°C)
0/100	71
90/10	42
80/20	45
60/40	46

The results are in agreement with those we have found in previous articles.[20–22]

The calorimetric results indicate that the HDPE/OBP blends form a partially miscible system containing at least three phases, two amorphous phases, one rich in HDPE with some OBP molecules, another rich in oligomer with some HDPE molecules and a third of crystalline HDPE.

The samples were kept in liquid nitrogen for 30 min, and then immediately broken and studied by SEM observation. As expected, the relief of the broken area of the HDPE surface reveals ductile fracture. Some voids observed were attributed to the formation and coalescence of microcavities, crack propagation and rupture by shearing. For all blends, the rough aspect of the relief of the fractured area indicates the occurrence of ductile fracture independent of the amount of OBP, as illustrated in Figure 5 (X1500). This photomicrograph shows small white points dispersed on the observed area, revealing some segregation. The occurrence of phase separation is shown in Figure 6 (X10000). The photomicrograph shows that HDPE is the matrix (see the black arrow on the photo), which reveals the occurrence of ductile fracture by shearing. The OBP phase (see the white arrow in dark region on the photo) is represented as dispersed domains surrounded by the HDPE matrix. The shape is variable, elongated and circular, and the size changes from

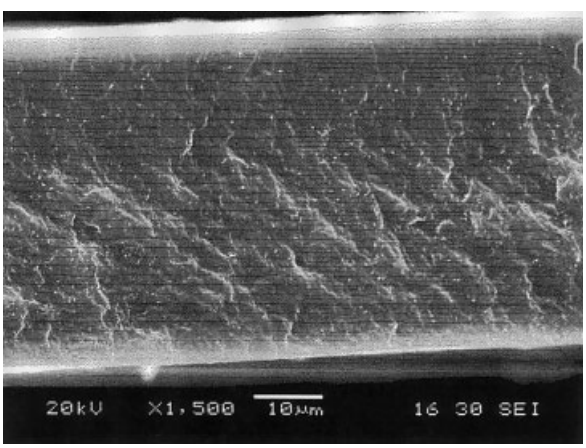

Figure 5 SEM photomicrograph of 60/40 HDPE/OBP film (×1500).

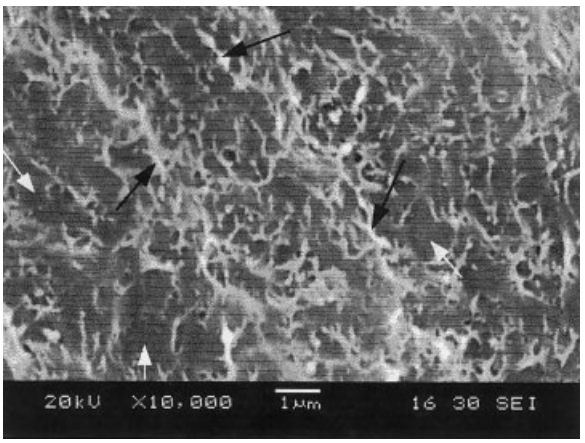

Figure 6 SEM photomicrograph of 60/40 HDPE/OBP film (×10000).

approximately 1 μm to smaller sizes. It seems to be closely connected to the polyolefin matrix. The white points in Figure 5 represent strands of HDPE (see dotted circle in Fig. 7, X30000) inserted in the OBP dispersed domain that underwent plastic deformation during the breaking process. SEM observations corroborate the results of thermal analysis.

The results of CO_2 permeability of HDPE/OBP blend films are listed in Table III. The gas permeability values of neat HDPE and 90/10 HDPE/OBP blend were similar. When the oligomer enriched the blend, the permeation value increased compared to plain HDPE, showing that the presence of oligomer affects the transport properties of the films. A progressive decrease in overall crystallinity in the blends was detected, indicating that the sorption and diffusion process of CO_2 through the films slightly increased and led to a loss in barrier property. If we consider the crystallinity of HDPE to remain practically unchangeable in the blends, with a value of 64%, it is possible to

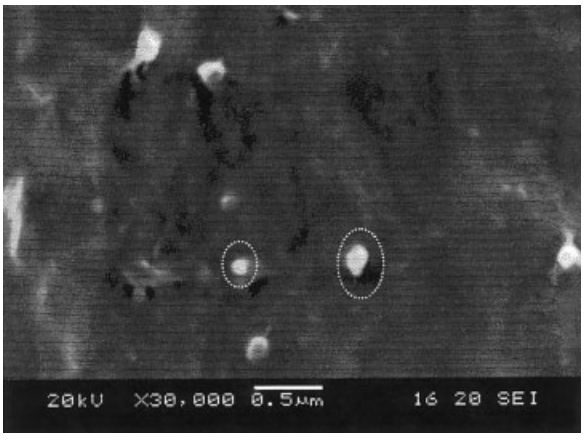

Figure 7 SEM photomicrograph of 60/40 HDPE/OBP film (×30000).

TABLE III
Permeability to CO_2 of HDPE/OBP Films

HDPE/OBP	$P \times 10^{10}$ cm^3 · cm/cm^2 · s · cmHg
100/0	1.76
90/10	1.76
80/20	1.90
60/40	2.48

evaluate the effect of OBP on permeability. In Table IV, we list the percentage of plain HDPE and blends in terms of crystalline and amorphous phase compositions. When we compare the composition of plain HDPE to that of the 60/40 HDPE/OBP blend, we detect a decrease of the crystalline portion from 64 to 38%. The difference represents almost twice the initial crystallinity. In contrast, in that blend 62% represents the amorphous portion of the sample, also almost twice the initial value of the amorphous phase in plain HDPE. Generally, the polymer crystalline phase is a barrier to gas diffusion, and permeation takes place only in the amorphous phase. This marked increase of the amorphous portion in the blend must cause a great increase in permeability, but the value registered was only slightly larger than that of plain HDPE. We must take into account the fact that, at the temperature of the test, the OBP rich phase is glassy, and the rigid domains of this phase could be acting as somewhat of a hindrance to the diffusion process through the blend film. Then the effect of loss in the overall crystallinity is counterbalanced to some extent by the presence of the OBP rich phase. The results support those found for a PP/OBP system reported in a recent paper.[22]

CONCLUSIONS

The calorimetric results reveal that blends of HDPE/OBP form a partially miscible system containing two amorphous and one crystalline phase. Plain HDPE presents a single, unique T_g, but in the blends, two transitions were observed. Besides the T_g of HDPE, another transition was detected and attributed to γ-transition of HDPE. The T_g ascribed to the amorphous OBP phase was practically independent of the

TABLE IV
Composition of Blends in Terms of Amorphous and Crystalline Portions

HDPE/OBP	OBP amorphous (%)	HDPE amorphous (%)	HDPE crystalline (%)
100/0	—	36	64
90/10	10	32	58
80/20	20	29	51
60/40	40	22	38

content of oligomer, with a value of about 45°C. The HDPE crystallized in all samples, causing a decrease in melting temperature and keeping the degree of crystallinity practically constant. The permeation of CO_2 showed a slight increased for 60/40 HDPE/OBP blend; meanwhile the 90/10 blend showed value similar to that of neat HDPE. The loss in overall crystallinity of the blends was counterbalanced to some extent by the presence of the OBP rich phase and could explain the variation observed in permeability.

NOMENCLATURE

P	permeability coefficient; (cm^3 cm/cm^2 s cm Hg)
l	film thickness; (cm)
dp/dt	gradient of the linear region (steady-state gas flow) of the pressure versus time plot; (cm Hg/s)
Δp	pressure difference between the two film sides; (cm Hg)
A	film area; (cm^2)
V_{syst}	volume system; (cm^3)
T_{amb}	temperature of test; (296 K)
T_{STP}	absolute temperature; (273 K)
P_{STP}	absolute pressure (76 cm Hg)

The authors thank the Coordination of University Level Staff Development (CAPES) of Brazil and the National Council of Scientific and Technological Development (CNPq) of Brazil for supporting this research. Also thank Antonio A. Ferreira, Jurandir M. de Souza and Angela C. P. Ferreira, technical staff of Petroflex, Brazil, for the help in DSC analysis at low temperature.

References

1. Schlademann, J. A. In Handbook of Pressure Sensitivfe Adhesive Technology; Satas, D., Ed.; Vamm Nostrand Reinhold: New York, 1982; p 353.
2. Roff, W. J.; Scott, J. R. In Fibres, Films, Plastics and Rubbers; Butterworth: London, 1971; pp 59–65, 237.
3. Findlay, J. In Encyclopedia of Polymer Science Technology; Mark, H. F., Gaylord N. G., Bikales N. M., Eds.; John Wiley & Sons: New York, 1968; Vol. 9, p 853.
4. Booth, A. B.; Autenrieth, J. S. In Encyclopedia of Chemical Technology; Mark, H. F., Mcketta Jr., J. J.; Othmer, D. F., Eds.; John Wiley & Sons: New York, 1969; Vol. 19, p 803.
5. Turreda, L. D.; Sekiguchi, Y.; Takemoto, M.; Kajiyama, M.; Hatano, Y.; Mizamachi, H. J Appl Polym Sci 1998, 70, 409.
6. Kim, J. K.; Ryu, D. Y.; Lee, K-H. Polymer 2000, 41, 5195.
7. Ryu, D. Y.; Kim, J. K. Polymer 2000, 41, 5207.
8. Akiyama, S.; Kobori, Y; Sugisaki, A.; Koyama, T.; Akiba, I. Polymer 2000, 41, 4021.
9. Cimmino, S.; Di Pace, E.; Martuscelli, E.; Mendes, L. C.; Silvestre, C.; Bonfanti, G. J J Polym Sci Part B: Polym Phys 1995, 33, 1723.
10. Cimmino, S.; Di Pace, E.; Martuscelli, E.; Mendes, L. C.; Silvestre, C. J Polym Sci Part B: Polym Phys 1994, 32, 2025.
11. Mendes, L. C.; Mano, E. B.; Martuschelli, E.; Cimmino, S. Polym Bull 1995, 35, 237.
12. Mendes, L. C.; Tavares, M. I. B; Mano, E. B. Polym Testing 1996, 15, 53.
13. Cardoso, R. S.; Simões, A. L. C.; Diez Filho, M. A.; Mendes, L. C. Polym Bull 1998, 40, 779.
14. Cardoso, R. S.; Simões, A. L. C.; Mendes, L. C.; Teixeira, S. C. S.; Ferreira, A. A. Polym Bull 1998, 40, 787.
15. Mendes, L. C.; Cardoso, R. S.; Chagas, B. S.; Moraes, G. F. Intern J Polym Mat 2000, 46, 801.
16. Mendes, L. C.; Cardoso, R. S.; Chagas, B. S.; Oliveira, M. L. C.; Moraes, G. F. Intern J Polym Mat 2000, 46, 395.
17. Tavares, M. I. B.; Mendes, L. C.; Cardoso, R. S.; Sanches, N. B.; Chagas, B. S. Intern J Polym Mat 2000, 46, 793.
18. Cimmino, S.; D'Alma, E.; Di Lorenzo, M. L.; Di Pace, E.; Silvestre, C. J Polym Sci Part B: Polym Phys 1999, 37, 867.
19. Di Lorenzo, M. L.; Cimmino, S.; Silvestre, C. Macromolecules 2000, 33, 3828.
20. Mendes, L. C.; Martins, B. B. B.; Dias, M. L.; Chagas B. S. Mat Res Innovat 2001, 4, 360.
21. Mendes, L. C.; Martins, B. B. B. Polym & Polym Composites 2002, 10, 183.
22. Mendes, L. C.; Miranda, F. C.; Ferreira, A. F.; Dias, F. M.; Garcia, M. E. F. J Appl Polym Sci, to appear.
23. American Society for Testing and Materials, ASTM D 792.
24. Pereira, C. C.; Souza, J. M. N.; Nobrega, R.; Borges, C. P. J Appl Polym Sci 2001, 81, 908.
25. Teo, L-S.; Kuo, J-F.; Chen, C-Y. Polymer 1998, 39, 3355.
26. Quirk, R. P.; Alsamarraie, M. A. A. In Polymer Handbook; Brandrup, J., Immergut, E. H., Eds.; John Wiley & Sons: New York, 1989; p V-15.
27. Beatty, C. L.; Karasz, F. E. J Macromol Sci Rev Macromol Chem 1979, C17, 37.
28. Lee, S.; Simha, R. Macromolecules 1974, 7, 909.
29. Stehling; F. C.; Mandelkern, L. Macromolecules 1970, 3, 242.
30. Beach, D. L.; Kissin, Y. V. In Encyclopedia of Polymer Science and Engineering; Mark, H. F.; Bikales, N. M.; Overberger C. G.; Menges, G., Eds; John Wiley & Sons: New York, 1986; Vol. 6, p 383.